

# WAVE BREAKING AND TEST PARTICLE DYNAMICS IN INHOMOGENEOUS BEAMS\*

R. P. Nunes<sup>†</sup>, F.B. Rizzato<sup>‡</sup>, R. Pakter<sup>§</sup>, Y. Levin<sup>¶</sup>, and E. G. Souza<sup>||</sup>  
Instituto de Física, Universidade Federal do Rio Grande do Sul  
Caixa Postal 15051, 91501-970, Porto Alegre, RS, Brazil

## Abstract

In this work, we analyze the dynamics of inhomogeneous, magnetically focused high-intensity beams of charged particles. While for homogeneous beams the whole system oscillates with a single frequency, any inhomogeneity leads to propagating transverse density waves which eventually result in a singular density build up, causing wave breaking and jet formation. Jets expell particles from the beam core and ultimately generate a halo of particles with concomitant emittance growth. Emittance growth directly indicates when the beam relaxes to its final stationary state, and the purpose of the present paper is to describe halo and emittance in terms of test particles moving under the action of the inhomogeneous beam. To this end we develop an average Lagrangian approach for the beam which produces results very similar to those obtained with full  $N$ -particle beam numerical simulations.

## INTRODUCTION

It is well known that magnetically focused beams of charged particles can relax from non-stationary into stationary flows with the associated particle evaporation [1]. Gluckstern [2] showed that initial oscillations of mismatched beams induce formation of large scale resonant islands [3, 4] beyond the beam border: beam particles are captured by the resonant islands resulting in emittance growth and relaxation. A closely related question concerns the mechanism of beam relaxation and the associated emittance growth when the beam is not homogeneous. On general grounds of energy conservation one again concludes that beam relaxation takes place as the coherent fluctuations of beam inhomogeneities are converted into microscopic kinetic energy [1, 5].

Recent investigation shows that relaxation comes about as a consequence of breaking of density waves followed by ejection of fast particle jets [6]. Jets are formed by particles moving in-phase with the macroscopic density fluctuations. They draw their energy from the propagating wave fronts and convert it into microscopic kinetic energy. For strongly inhomogeneous beams, we find that it is the wave breaking and jet production which are the primary mechanisms responsible for the beam relaxation. Once some particles are

ejected from the beam core, they start to form a low density population which, precisely due to its low density, can be described as a set of test particles. One important feature in modeling the system is to give an accurate account of the core dynamics driving the test particles. To do that we make use of a Lagrangian approach which is described in the following.

## THE MODEL AND ANALYSIS

We consider solenoidal focusing of space-charge dominated beams propagating along the transport axis, defined as the  $z$  axis of our reference frame. The beam is initially cold with vanishing emittance and is azimuthally symmetric around the  $z$  axis. Our problem is then to describe the average oscillatory motion of the beam core and how it drives test particles to form halo with subsequent beam relaxation.

Considering full azimuthal symmetry, one can use Gauss's law in order to write the governing equation for any particle in the beam [7, 8, 9],

$$r'' = -\kappa r + \frac{Q(r)}{r}. \quad (1)$$

The prime indicates derivative with respect to the longitudinal  $z$  coordinate which for convenience we shall also refer to as "time". The focusing factor is  $\kappa \equiv (qB/2\gamma m\beta c^2)^2$ , where  $B$  is the axial, constant, focusing magnetic field;  $Q(r) = KN(r)/N_t$ , is the particle-averaged measure of the charge contained between the origin at  $r = 0$  and the position  $r(z) = r$ ,  $N_t$  is the total number of beam particles per unit axial length,  $N(r)$  is the number of particles up to  $r$ , and  $K = N_t q^2 / \gamma^3 m \beta^2 c^2$  is the beam perveance.  $q$  and  $m$  denote the beam particle charge and mass, respectively;  $\gamma = (1 - \beta^2)^{-1/2}$  is the relativistic factor where  $\beta = v_z/c$  and  $v_z$  is the constant axial beam velocity and  $c$  is the speed of light.

### Core Density Oscillations

In cold systems, particles in the core are approximately described in terms of a charged fluid where fluid elements do not crossover each other during the dynamics. Particles crossing over each other are halo particles and shall be handled later. Since the core is assumed to be a fluid, the amount of charge that a core particle sees at any time equals the charge it saw initially at  $z = 0$ . In other words, for a core particle at  $r_o$ ,  $Q(r) = Q(r_o)$ . At this point we note that the initial coordinate  $r_o$  is in fact the Lagrangian

\* CNPq and FAPERGS, Brazil; AFOSR-FA9550-06-1-0345, USA

<sup>†</sup> rogerpn@if.ufrgs.br

<sup>‡</sup> rizzato@if.ufrgs.br

<sup>§</sup> pakter@if.ufrgs.br

<sup>¶</sup> levin@if.ufrgs.br

<sup>||</sup> evertongs@if.ufrgs.br

coordinate of the the core particle [10], which means that the solution to Eq. (1) can be written parametrically in terms of  $r_0$ . Once again we emphasize that the amount of charge  $Q(r)$  seen by the fluid element inside the region  $0 < r \leq r(z)$  remains unaltered at  $r_0$ , independent of time  $z$ . This is of fundamental importance since from the Gauss law this is the charge that exerts the force on the fluid element.

Expression (1) can be readily obtained from the single-particle Lagrangian  $\mathcal{L}$

$$\mathcal{L}(r, r') = \frac{r'^2}{2} - \kappa \frac{r^2}{2} + Q(r_0) \ln(r), \quad (2)$$

with help of Euler-Lagrange equations. In our system one has a multitude of  $N_t$  particles, as mentioned, and the full Lagrangian takes the form

$$L = \int \mathcal{L}(r, r') n(r_0) d^2 r_0 dz, \quad (3)$$

where what one is doing is to multiply the single-particle Lagrangian at coordinate  $r$  by the number of particles evolving from  $r(z=0) = r_0$  to  $r(z) = r$ ,  $n(r_0)d^2 r_0$ , and integrating over all possible initial conditions.

This is the point where we would like to invoke average Lagrangean techniques [11]. We shall assume a trial shape for the density  $n = n(r, \eta(z))$ , integrate Eq. (2) over  $r$  and apply Euler-Lagrange method to obtain a governing equation for the density fluctuation amplitude  $\eta(z)$ . This will complete the description for the core dynamics. To achieve our goal we first of all note that given continuity, particles description through Eulerian or Lagrangian variables are constrained to  $n(r_0)d^2 r_0 = n(r)d^2 r$ . In addition to that, continuity can be used once again to extract an expression for the velocity  $r'$  in terms of the coordinate and time:

$$r' = -\frac{1}{r n} \int_0^r r \frac{\partial}{\partial z} n(r, z) dr \equiv v \quad (4)$$

where again we remember that axial symmetry has been assumed.

Now we need the *ansatz* for the density. As initial condition we impose a perturbation of the form  $n = \rho_h [1 + \eta(2r^2/r_b^2 - 1)] - \rho_h$  is the average beam density - and assume that as the density wave evolves it can be represented in the form

$$n(r, \eta(z)) = \rho_h \left[ 1 + \eta(z) \left( 2 \frac{r^2}{r_b^2} - 1 \right) \right], \quad (5)$$

where we allow the amplitude to become a function of time  $z$ . The *ansatz* represents a compressive-rarefactive wave which, given the initial condition, seems likely to occur in the system.

Finally, integration of Eq. (3) and use of Euler-Lagrange equations allows to obtain a closed form for the amplitude

$$\eta''(z) = F(\eta(z), \eta'(z)) \quad (6)$$

where the specific form of the very involved function  $F$  can be readily obtained from the Eule-Lagrange procedures, and shall be discussed in a future publication due to the several details of its obtention.

### Test particle orbits

As for the test particles, Eq. (1) is applied with restrictions on the argument of the charge function  $Q(r)$ , but assuming that this latter function contains only the core charge. This is equivalent to our assumptions on the diluteness of the halo.

Test particles inside the beam feel the space charge action of the core up to their actual position  $r = r(z)$ . Therefore the governing equation for those test particles can be written in the form

$$r'' = -\kappa r + \begin{cases} K \frac{r(r_b^2 + (r^2 - r_b^2)\eta(z))}{r_b^4} & \text{if } r \leq r_b \\ K/r & \text{if } r > r_b \end{cases} \quad (7)$$

Equations (6) and (7) shall be solved simultaneously to obtain the test particle dynamics.

## FULL AND TEST PARTICLE SIMULATIONS

In virtue of the complete integrability of the  $\eta$  dynamics, the test particle motion can be represented in terms of a convenient Poincaré plot, where we record the pair of values  $r(z)$  and  $r'(z)$  each time  $\eta' = 0$  with  $\eta'' < 0$ .

We also chose  $r_b = K/\kappa$  so particles at beam border are at equilibrium. One can picture the beam as displaying internal oscillations, but keeping its radius unaltered. This reduces the action of Gluckstern's resonances and therefore enhances the effects of density oscillations.

One can also rescale radiuses, perveance and focusing factor so as to work with  $K = \kappa = r_b = 1$  at equilibrium [12]. If in addition one selects  $\eta(0) = 0.6$  and  $\eta'(0) = 0$  as typical initial conditions at beam entrance, one obtains the dynamics for the test particles shown in the Fig. (1).

A full particle simulation is then performed, where each particle is governed by Eq. (1) and where now the charge factor  $Q(r)$  is *fully* and *self-consistently* evaluated with basis on all particles coordinates. Detailed information about the self-consistent method employed in the beam simulation shown here can be found in Ref. [13].

Results for this latter simulations are displayed in the panels of Fig. (2) where one sees all beam particles as they move in the phase-space. Of particular importance is the saturated situation, panel (e), attained at the beginning of the flat emittance line of panel (f). At this point the full particle population can be approximately divided into two subspecies: a cold high density core and a hot low density environment of higher energy particles. The geometric layout of the hot environment agrees quite well with results displayed on Fig. (2), which strongly suggests that modeling in terms of a cold core and a population of non

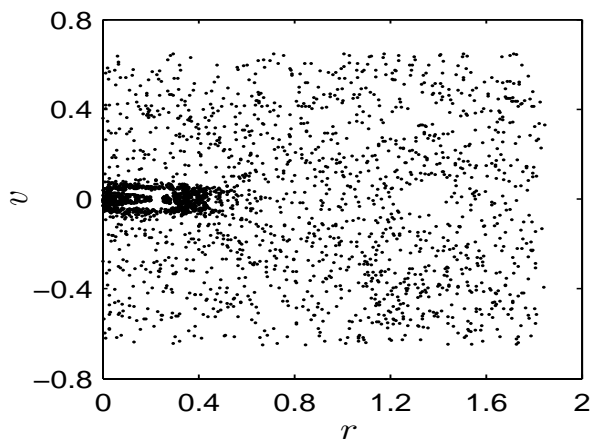


Figure 1: Test particle dynamics for  $\eta(0) = 0.6$ ,  $\eta'(0) = 0$ .

self-interacting test particles may be indeed very appropriate for the system. From this Fig. (2) one also sees in panel (c) the operations of the wave breaking mechanism, which rapidly progresses and unfolds in panel (d). The jets induce particles to abandon the core, which then populate a restricted rectangular-like region in the phase-space around the cold core. This behavior can be visualized in panel (e). These particles with velocities that cannot be neglected can be identified as the ones which will compose the halo in a inhomogeneous matched beam.

## FINAL REMARKS

Combining an average Lagrangian method, techniques of Lagrangian fluids, and test particle methods, we could obtain an accurate description of the geometric layout of halo in inhomogeneous beams. The inhomogeneous core undergoes wave breaking, and ejects a low density population of particles that move under the action of the core. The low density population is represented by test particles in our model. What remains to be done to fully complete this low dimensional modeling is to make use of conserved quantities in order to calculate the density of the halo. This has been done with success in the recent past [12] and is the goal we are currently pursuing.

## REFERENCES

- [1] A. Cuchetti, M. Reiser, and T. Wangler, in *Proceedings of the Invited Papers, 14<sup>th</sup> Particle Accelerator Conference*, San Francisco, USA, 1991, edited by L. Lizama and J. Chew (IEEE, New York, 1991), Vol. 1, p. 251.
- [2] R.L. Gluckstern, *Phys. Rev. Lett.* **73**, 1247 (1994).
- [3] R. Pakter, G. Corso, T.S. Caetano, D. Dillenburg, and F.B. Rizzato, *Phys. Plasmas*, **12**, 4099 (1994).
- [4] R. Pakter, S.R. Lopes, and R.L. Viana, *Physica D* **110**, 277 (1997).

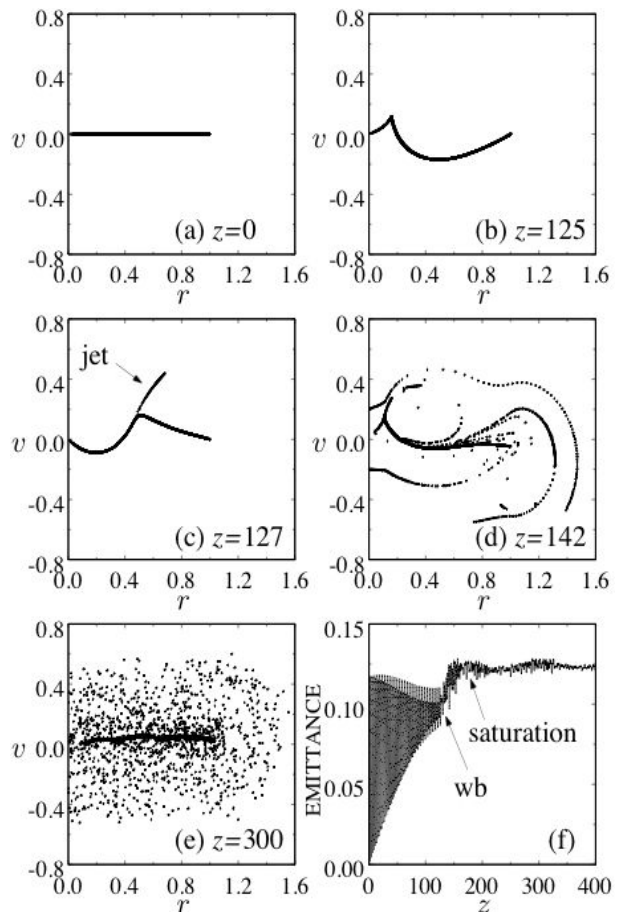


Figure 2: Full simulations displaying snapshots of the phase-space. Panel (e) represents the relaxed state and the last panel (f) offers a view of emittance growth and saturation.

- [5] S.M. Lund, D.P. Grote, and R.C. Davidson, *Nuc. Instr. and Meth. A* **544**, 472 (2005); Y. Fink, C. Chen and W.P. Marable, *Phys. Rev. E* **55**, 7557 (1997).
- [6] F.B. Rizzato, R. Pakter, and Y. Levin, *Phys. Plasmas* **14**, 110701 (2007).
- [7] H. Okamoto and M. Ikegami, *Phys. Rev. E* **55**, 4694 (1997).
- [8] M. Reiser, *Theory and Design of Charged Particle Beams*, (Wiley-Interscience, 1994); R.C. Davidson and H. Qin, *Physics of Intense Charged Particle Beams in High Energy Accelerators* (World Scientific, Singapore, 2001).
- [9] R. Pakter and F.B. Rizzato, *Phys. Rev. Lett.* **87**, (2001).
- [10] P.J. Morrison, *Rev. Mod. Phys.* **70**, 467 (1998).
- [11] G.B. Witham *Linear and Nonlinear Waves* Wiley, New York (1974).
- [12] R.P. Nunes, R. Pakter, and F.B. Rizzato, *J. App. Phys.* **104**, To be published (2008).
- [13] R.P. Nunes, R. Pakter, and F.B. Rizzato, *Phys. Plasmas* **14**, 023104 (2007).